Arabian Journal of Chemistry (2022) **15**, 103764

King Saud University

Arabian Journal of Chemistry

www.ksu.edu.sa
www.sciencedirect.com

ORIGINAL ARTICLE

Green synthesis of iron (Fe) nanoparticles using *Plumeria obtusa* extract as a reducing and stabilizing agent: Antimicrobial, antioxidant and biocompatibility studies

Shazia Perveen [a], Raziya Nadeem [a,*], Shafiq ur Rehman [a], Nosheen Afzal [b], Shazia Anjum [c], Saima Noreen [a], Rashid Saeed [d], Mongi Amami [e,f], Samiah H. Al-Mijalli [g,*], Munawar Iqbal [h,*]

[a] *Department of Chemistry, University of Agriculture, Faisalabad 38000, Pakistan*
[b] *Department of Biochemistry, Government College University, Faisalabad, Pakistan*
[c] *Department of Chemistry, The Islamia University of Bahawalpur, 63100 Bahawalpur, Pakistan*
[d] *Department of Environmental Sciences, University of Gujrat, Gujrat, Pakistan*
[e] *Department of Chemistry College of Sciences, King Khalid University, P.O. Box 9004, Abha, Saudi Arabia*
[f] *Laboratoire des matériaux et de l'environnement pour le développement durable LR18ES10, 9 Avenue Dr.Zoheir Safi, 1006 Tunis, Tunisia*
[g] *Department of Biology, College of Sciences, Princess Nourah bint Abdulrahman University, P.O. Box 84428, Riyadh 11671, Saudi Arabia*
[h] *Department of Chemistry, Division of Science and Technology, University of Education, Lahore, Pakistan*

Received 11 September 2021; accepted 1 February 2022
Available online 7 February 2022

KEYWORDS

Biosynthesis;
Iron nanoparticles;
Biocompatibility;
Antioxidant;
Cytotoxicity;
Antimicrobial;
Antioxidant activity

Abstract In the current study, a green and facile route for the synthesis of iron nanoparticles (FeNPs) was adopted. The FeNPs were fabricated via a single step green route using aqueous leaves extract of *Plumeria obtusa* (*P. obtusa*) as a capping/reducing and stabilizing agents. The FeNPs were characterized by UV/Vis (Ultraviolet/Visible), FTIR (Fourier Transform Infra-Red spectroscopy), TEM (Transmission Electron Microscopy), SEM (Scanning Electron Microscopy) and XRD (X-Ray Diffraction) techniques. The FeNPs were of spheroidal shape with average size of 50 nm. The biosynthesized FeNPs were further evaluated for their biological activities like antimicrobial, antioxidant and biocompatibility. The FeNPs displayed auspicious antimicrobial activity against

* Corresponding authors.
E-mail addresses: raziyaanalyst@yahoo.com (R. Nadeem), Shalmejale@pnu.edu.sa (S.H. Al-Mijalli), bosalvee@yahoo.com (M. Iqbal).
Peer review under responsibility of King Saud University.

Production and hosting by Elsevier

https://doi.org/10.1016/j.arabjc.2022.103764

bacterial (*E. coli*, *B. subtilis*) and fungal strains (*A. niger*) and *S. commune*. The test performed against red blood cells (RBCs) lysis (1.22 ± 0.02%) and macrophage (31 ± 0.09%) showed biocompatible nature of FeNPs. *In vitro* cytotoxicity against AU565 (82.03 ± 0.08–23.65 ± 0.065 %) and HeLa (88.61 ± 0.06–33.34 ± 0.06%) cell lines showed cell viability loss in dose dependent manner (FeNPs 25–100 µg/mL). The antioxidant activities values were determined through DPPH, TRPA, NO and H_2O_2 assays with values 70.23 ± 0.02%, 76.65 ± 0.02 µg AAE/mg, 74. 43 ± 0.04% and 67.34 ± 0.03%, respectively. Based on the bioactivities, the green synthesized FeNPs have potential for therapeutic applications.

1. Introduction

In current era, nanotechnology has become most interesting approach primarily concerned with preparation and utilization of materials in nano range (1–100 nm). Metal nanoparticles (NPs) display exceptional attributes and higher surface area due and have potential application in numerous fields including food, sensors, optics, electronics, catalysis, agriculture, paints, cosmetics, batteries, drug delivery and most importantly in medicine (Nadeem et al., 2021; Nazir et al., 2021; Rahmat et al., 2021). Among different metal NPs, iron nanoparticles (FeNPs) have attracted much attention of the researchers owing to their promising bioactivates and non-toxic nature (Igwe and Nwamezie, 2018). The FeNPs have wide applications in various commercial fields comprising; radiology, bio-medicine, cosmetics, diagnostics, enzymes, pathogens sensor, vaccines and antigen detection due their unique attributes like higher surface area, high stability and smaller band gap (2.1 eV) (Ruan et al., 2018; Bibi et al., 2019; Bhatti et al., 2020; Noreen et al., 2020).

For the fabrication of FeNPs, diverse physicochemical approaches and biological routes have been employed. The physicochemical techniques have various disadvantages like use of reducing agents, expensive metal salts, organic solvents and beside this, they need higher temperature consume energy, need chemical additives and costly instruments (Bhatti et al., 2020; Noreen et al., 2020). Hence, aforementioned approaches are not only costly at industrial scale, the NPs prepared using these approaches cannot be utilized in medicines as well because of their toxic nature of chemical used during the preparation of NPs. In order to overwhelm these limitations, it is need of time to develop safer, cleaner as well as sustainable approach for synthesis of NPs. The biosynthesis approach attracted much attention in this regard due to its eco-friendly nature and cost effectiveness as well as potential applications of NPs in the medical field (Igwe and Nwamezie 2018; Bibi et al., 2019; Noreen et al., 2020).

The synthesis of metal NPs utilizing biological sources like fungi, plants, algae, bacteria, diatoms and yeast has many advantages over other conventional techniques since no harmful byproduct is involved (Kamran et al., 2019; Naseer et al., 2020; Ali et al., 2021). The main drawback connected to microbial source is the maintenance of culture media, intensive isolation cost and contamination free environment (Kamran et al., 2019). Thus, plants extract (phyto-fabrication) proved to be potential reducing agent in NPs fabrication. The plants extract comprised of various bioactive molecules like alkaloids, phenolic, tannins, flavonoids, saponins, amino acids, vitamins, terpenes and inositol, reduce and stabilize the ions to metal atom (Al Banna et al., 2020; Awwad et al., 2020; Al-Fa'ouri et al., 2021; Amer and Awwad 2021; Shammout and Awwad 2021). *Plumeria obtusa* is commonly known as Gulechin or Graveyard belonging to family *Apocynaceae*. The genus *Plumeria* (*Apocynaceae*) comprises of eight species growing in subtropical and tropical regions. Different species of this genus are being used as medicine for treatment diarrhea, syphilis, gonorrhea, leprosy and veneral sores. Two species namely Plumeria obtusa and Plumeria rubra are grown in Pakistan for ornamental purposes (Bihani 2021a and 2021b). Plumeria obtusa is well known for its wide availability in Pakistan. This plant contains flavonoids such as quercetin, naringenin, kaempferol, mixed fatty acids, gallic acid, chrysophanol, triterpenoids, champalinol, champalin A, champalinone, 8-sterols, champalin and due to these constituents, this plant possesses antimicrobial and antioxidant potentials, which is used in the treatment of asthma, constipation, diabetes mellitus, anti-inflammatory, antimicrobial, activities, cure of respiratory ailments and gonorrhea. It is also used as a expectorant, contraceptive and anthelmintic drug (Bihani 2021a and 2021b).

Based on aforementioned facts, in the current study, we reported an ecofriendly and facile route for the bio-reduction of ferrous acetate ($Fe(CH_3CO_2)_2$) using *P. obtusa* leaf extract without utilizing surfactants, inorganic and organic solvents. The biosynthesized FeNPs were studied employing techniques like FTIR, UV/Vis, SEM and TEM. In addition, the biocompatibility, antimicrobial and antioxidant activities of biosynthesized FeNPs were also evaluated.

2. Material and methods

2.1. Reagents/chemicals

The chemicals/reagents used of analytical grade, including ferrous acetate ($Fe(C_2H_3O_2)_2$), deionized water, dimethyl sulfoxide (DMSO), streptomycin, sabouraud dextrose, Fluconazole, resazurin indicator, DPPH, ascorbic acid (AA) ($C_6H_8O_6$), ferric chloride hexahydrate ($FeCl_3$: $6H_2O$), butylated hydroxyl toluene (BHT), sodium nitroprusside, fresh human blood, ethylene diamine tetra acetate (EDTA), phosphate-buffer saline (PBS), Triton X-100, MTT, Doxorubicin and Cisplatin, Hela cells and AU565 cell lines, DMEM reagent, bovine serum, penicillin. The *Escherichia coli* and *Bacillus subtilis, Aspergillus niger* and *Schizophyllum commune* pure cultures were obtained from Biochemistry Laboratory, University of Agriculture Faisalabad.

2.2. Extract preparation

The *P. obtuse* fresh leaves were taken University of Agriculture Faisalabad, Pakistan (Botanical Garden). The leaves were properly rinsed using water for cleaning purpose. A 20 g fresh leaves of *P. obtusa* were used into 100 mL of deionized water to prepare extract. The mixture was stirred continuously and heated at 80 °C for ~60 min. The resulting solution was cooled down, filtered and extract was preserved at 4 °C for further use in bio-fabrication of FeNPs (Halanayake et al., 2021).

2.3. Bio-fabrication of FeNPs

The FeNPs were fabricated by adding 50 mL of 3 mM solution of ferrous acetate ($Fe(C_2H_3O_2)_2$) into 100 mL of extract of *P.*

obtusa. The contents was heated at 70 °C for 2 h with continuous stirring, while keeping the pH of solution at 9.0 using NH_4OH solution. Then, it was cooled down, centrifuged (3000 rpm) for 20 min. The FeNPs were rinsed with deionized water many times to eliminate residues of *P. obtusa* leaves extract residues and ions. The resulting powdered was incubated for 2 h at 75 °C and the calcination of FeNPs was performed at 600 °C (Iqbal et al., 2020), which were further subjected to characterization and bioactivity evaluation. The biosynthesis study plan is shown in Fig. 1.

2.4. Characterization of FeNPs

The biosynthesized FeNPs were subjected to different characterization techniques UV/Vis spectroscopy (UV-4000 spectrophotometer, Germany), FTIR (Alpha, Bruker, Germany) using the KBr method (0.002 g sample was grinded with 0.98 g KBr). The XRD of FeNPs was investigated using X-ray diffractometer (Bruker Germany, BRUKE-D8-ADVANCE) at current voltage of 40 mA and Cu Kα radiations source energized at 45 kV ($\lambda = 0.15418$ nm) in a diffraction angle range of 2θ from 10° to 80°. The SEM (NOVAFEISEM-450) and TEM (JEOL 2000 FX) for morphological analysis of the FeNPs using at voltage of 10–15 kV and analysis was carried out using Image J software for SEM. The UV/Vis spectra were observed in the range of 200–800 nm wavelength. FTIR analysis was performed in range of 500–4500 cm^{-1} to characterize potential bioactive responsible for the reduction of metal ions to atom. The average crystalline size of NPs was recorded using crystallite size calculator (Scherrer formula) (Bihani et al., 2021; Halanayake et al., 2021).

2.5. Antimicrobial activity evaluation

2.5.1. Sample preparation

The biosynthesized FeNPs were elucidated for their biological activities. The colloidal suspensions were prepared for this purpose by addition of 1 mg FeNPs to 1 mL of dimethyl sulfoxide (DMSO) and sonicated for about 30 min. Furthermore, colloidal suspension stability was investigated by adding 3 mg FeNPs into 3 mL of DMSO and resulting slight turbidity, which was allowed to stand in order to observe the UV-spectra to check stability.

2.5.2. Antibacterial activity

The antibacterial potential of FeNPs was explored against *E. coli* and *B. subtilis*. For this, bacterial culture was multiplied and refreshed into test tubes having media (nutrient broth) and was kept in incubator (PA225/25H) at 37 °C for 24 h and 240 rpm. The cotton swaps were used to spread the bacterial strains onto media plates. To evaluate antibacterial activities, the agar well diffusion method was employed. The filter discs (6 mm each) laden with 10 µL of FeNPs (with dilution 20–100 µg/mL) were dried and kept on bacterial lawns in order to avoid the spread of FeNPs suspension. A 10 µL of streptomycin was used as a positive control. Subsequently, all the petri plates are placed at 37 °C/24 h and inhibition zone of estimated using zone reader (Abbasi et al., 2019).

2.5.3. Antifungal activity

The antifungal capacity of FeNPs was explored against *A. niger* and *S. commune* applying disc-diffusion method (Iqbal et al., 2020). The spores of fungus were cultured in conical flasks (100 mL) comprising liquid media (sabouraud dextrose) and placed into the incubator for 24 h at 25 °C. The sabouraud dextrose media was autoclaved and then, transferred into the petri plates (sterilized). In order to homogenize fungal spores, 50 µL of broth medium culture was spread on the petri plates by using autoclaved cotton swab. A 10 µL FeNPs were loaded to each petri plate. The DMSO and Fluconazole served as negative and positive controls. Furthermore, fungal plates were incubated for 24 h/25 °C and inhibition zones were observed after this time period. The FeNPs concentrations were studied in 20–100 µg/mL range.

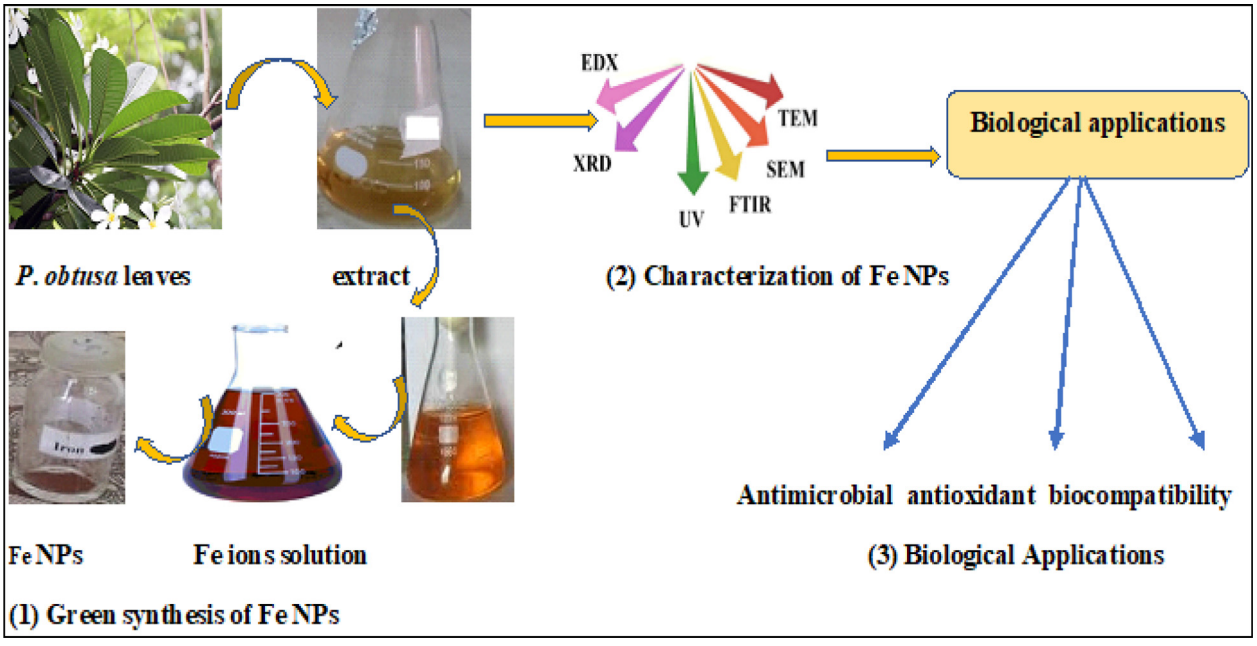

Fig. 1 Schematic presentation of biosynthesis of FeNPs using *P. obtusa* extract and applications.

2.5.4. Minimum inhibitory concentrations (MICs)

Microdilution method was used for MICs determination. Liquid culture medium was employed for serial dilution of FeNPs suspension in 96 well plate. After incubation, 0.2 mg/mL resazurin indicator (10 µL) was added into each well and incubated for 30 min. The presence of live bacteria was indicated by the appearance of pink color. The inoculums concentration were kept 10^5 spores/mL and each well has 10^6 CFU/mL. The FeNPs different concentrations (50–500 µg/mL) were used for MIC study. The optical density was recorded at 510 nm in case of bacteria, while at 620 nm for fungus and values were expressed as µg/mL and all runs were performed in triplicate (Patil Shriniwas, 2017).

2.6. Antioxidant activity evaluation

To elucidate free radical scavenging potential of FeNPs, the spectrophotometric method was used according to protocol reported elsewhere (Hamelian et al., 2018). For this purpose, DPPH (2.4 mg) was added into 25 mL CH_2OH and vortexed properly. Later on, FeNPs with different concentrations ranging from 25 to 500 µg/mL were utilized to explore their free radical quenching capacity. The standards used in this assay were ascorbic acid (AA) (positive control) and DMSO (negative control). The 200 µL reaction mixture containing 20 µL FeNPs and 180 µL reagent solution was laden into 96-well Eliza plate and incubated for 1 h in dark. After that the absorbance was monitored at 517 nm via reader (microplate). The % scavenging of DPPH was determined using following equation.

$$\text{DPPH scavenging } (\%) = 1 - \left[\frac{\text{Sample absorbance}}{\text{control absorbance}}\right] * 100 \quad (1)$$

The total reducing power ability of FeNPs was performed using $K_3[Fe(CN)_6]$ according to method (Abbasi et al., 2019) with slight modification. The DMSO and ascorbic acid (AA) served as negative and positive controls. A 200 µL of FeNPs were taken in different concentration ranging from 25 to 250 µg/mL. To each solution of FeNPs, 5 mL of phosphate buffer (6.6 pH) with 0.2 M concentration and 2.5 mL $K_3[Fe(CN)_6]$ (1%) were added and incubated the resulting solution for 30 min. After 30 min, 2.5 mL solution of $C_2HCl_3O_2$ (10%) was poured and then, centrifuged (3000 rpm) for 15 min. The upper layered 2.5 mL solution was mixed with 0.5 mL $FeCl_3$ (0.1%) and 2.5 mL water (deionized) and then, absorbance is monitored (630 nm). The reducing power is presented in terms of µg ascorbic acid equivalent per mg (µg AAE/mg) of NPs.

The hydrogen peroxide (H_2O_2) radical scavenging activity was evaluated utilizing FeNPs (25–500 µg/mL) and ascorbic acid as standard. A 200 µL FeNPs were mixed with 5 mM H_2O_2 solution and incubated for half an hour at room temperature and Eliza reader was employed for absorbance analysis at 610 nm. To compare the antioxidant capacity of FeNPs, the DMSO (negative control), while AA was employed as a positive control. The results were determined as µg AAE/mg of FeNPs by following the protocol (Khalil et al., 2017).

Nitric oxide (NO) scavenging potential of FeNPs was monitored taking different concentration (25–250 µg/mL) and butylated hydroxyl toluene (BHT) used as standard. Each concentration of FeNPs was mixed with equal volume of 20 mM freshly prepared sodium nitroprusside and the resultant solution incubated for 90 min at 25 °C. The optical density was recorded at 546 nm and radical scavenging activity was calculated (Sangaonkar and Pawar, 2018).

2.7. Biocompatibility and cytotoxicity evaluation

The biocompatibility assay of synthesized FeNPs was performed against human RBCs. The haemolytic activity was conducted using human RBCs (Abbasi et al., 2019). For this assay, 1 mL fresh human blood was taken into tube containing EDTA and subsequently, centrifuged for 15 min at 13,000 rpm. After that, the supernatant was discarded and pallets were washed thrice with phosphate-buffer saline (PBS). The suspensions of erythrocytes were prepared by adding 9.8 mL to PBS 200 µL erythrocytes. Then, 100 µL of erythrocytes suspension was mixed to different concentrations of FeNPs, incubated for 1 h/35 °C and centrifuged for 10 min at 10,000 rpm. The supernatants were shifted to 96-wells plate and the hemoglobin released was analyzed at 540 nm. PBS and Triton X-100 served as negative and positive controls. The hemolysis (%) was estimated by employing the Eq. (2).

$$\text{Hemolysis } (\%) = \left[\frac{\textit{Sample absorbance} - \textit{negative control absorbance}}{\textit{positive control absorbance} - \textit{negative control absorbance}}\right] * 100 \quad (2)$$

In addition, the human macrophage was also utilized to test biocompatibility of FeNPs by MTT assay. This assay is relayed on colorimetric detection using 96 well flat bottom micro plate integrated with cultured cells (100 µL/well) having 5×10^4 cells/mL concentration. Medium was replaced with 200 µL fresh medium after overnight incubation and to this, 200 µL of FeNPs with different concentrations (30–100 µg/mL) were added and the resulting medium again incubated for 2 days. Insoluble crystals of formazan were formed after addition of 200 µL of MTT (0.5 mg/mL) into this medium, which was kept at 37 °C for 4 h. Multichannel well plate used to remove excess bulk medium without disturbing formazan crystals. These NPs were dissolved by addition of 100 µL DMSO in each well, which further 15–20 min agitated followed by immediate measurement of absorbance at 570 nm with 650 nm reference wavelength. Doxorubicin and Cisplatin were used as standards, whereas positive control (without sample) served as 100% and 50% inhibition in growth (IC_{50}) of cell lines caused by specific concentration termed as cytotoxicity (Rolim et al., 2019). The percent inhibition was determined as shown in Eq. (3).

$$\text{Inhibition } (\%) = 100 - \left[\frac{\textit{Sample absorbance}}{\textit{positive control absorbance}}\right] * 100 \quad (3)$$

Hela cells and AU565 breast carcinoma cells were individually employed to assess cytotoxicity of synthesized FeNPs. The DMEM (Dulbecco's Modified Eagle Medium) having pH 7.2 was implemented for cells growth along with fetal bovine serum (5%), 100 IU/mL penicillin and 100 µg/mL streptomycin taken in 75 cm^2 which further incubated with 5% CO_2 atmosphere at room temperature (Nadhe et al., 2020).

2.8. Statistical analysis

The standard and means deviation (±S.E) of the three replicates was calculated. Statistical Package for Social Science Version 20.0 and Microsoft Office Excel Version 2010 was used for analysis. The ANOVA method followed by Duncan's multiple range test at $P < 0.05$ was applied to analyze the significant differences of the experimental data (Li et al., 2020).

3. Results and discussion

3.1. Characterization

The fabrication of FeNPs from ferrous acetate ($Fe(C_2H_3O_2)_2$) using leaves extract of *P. obtuse* was performed. The Fe $(C_2H_3O_2)_2$/*P. obtusa* solution color changed gradually at 70 °C to reddish black from dark brown, which is a signal of FeNPs formation. The color change was the preliminary confirmation for the bioreduction of Fe ions this, which was also confirmed by estimating the absorbance and the vibration of surface plasmon (Iqbal et al., 2020). The fabrication of FeNPs in an aqueous media was elucidated via UV/Vis spectroscopy by scanning the solution in 200–800 nm range. The maximum absorbance (λ_{max}) was observed 331 nm (Fig. 2) confirming the synthesis of FeNPs that was within range of surface plasmon resonance of Fe, which is consistent with previous reports (Iqbal et al., 2020). The additional peaks appeared in UV/Vis spectra are due to biomolecules present in the extract, these peaks are due to π/π^* transitions confirming the occurrence of aromatic compounds in the extract.

The FT-IR analysis was employed for the analysis of possible biomolecules and functional molecules responsible for biosynthesis. Fig. 3 indicates FTIR spectra of *P. obtusa* and biosynthesized FeNPs, respectively. The broad band was analyzed corresponding to the phenol functional group, N-H/C-H/O-H stretching bonding of amines, amides, —COOH, C-N groups was observed between 3503 and 2019 cm^{-1} range. The presence of carbonyl functional groups was attributed to small peak at 1769 cm^{-1}, while a strong peak was seen at 1620 cm^{-1} due to stretching of C=C. There were other peaks particularly observed at 1481, 1308, 1182 and 663 (cm^{-1}), which are related to the aliphatic ether. However, in case of FeNPs. The bands appearing in spectra of FeNPs at 3556–3254, 2165, 1655, 1434, 1307, 1174 (cm^{-1}) are due to the O—H, C—H, C—N, C—O and S=O of aromatic ester vibrations. The band at 621 cm^{-1} showed the existence of Fe—O bond vibration. There was remarkable shifting of peaks in plant mediated FeNPs, thus suggesting participation of respective functional groups in reduction process and FeNPs formation. FT-IR studies revealed that synthesized FeNPs possessed biomolecules of *P. obtusa* extract. The distinct and significant IR peaks of these biomolecules were present in the IR spectra of synthesized FeNPs. As the Fe^{+3} reduced upon interaction of ferric acetate with leaves extract of *P. obtusa*. Previous reports also revealed the presence of bioactive compounds, i.e., quercetin, gallic acid, kaempferol, chrysophanol, naringenin, etc.) in plant extracts (Yadav and Fulekar, 2018; Al Banna et al., 2020; Awwad and Amer, 2020), which are responsible for reduction metal ions to metal stable atom. These biomolecules bind to metal ions surface and play substantial role in reducing and stabilizing the NPs. The bioactive molecules

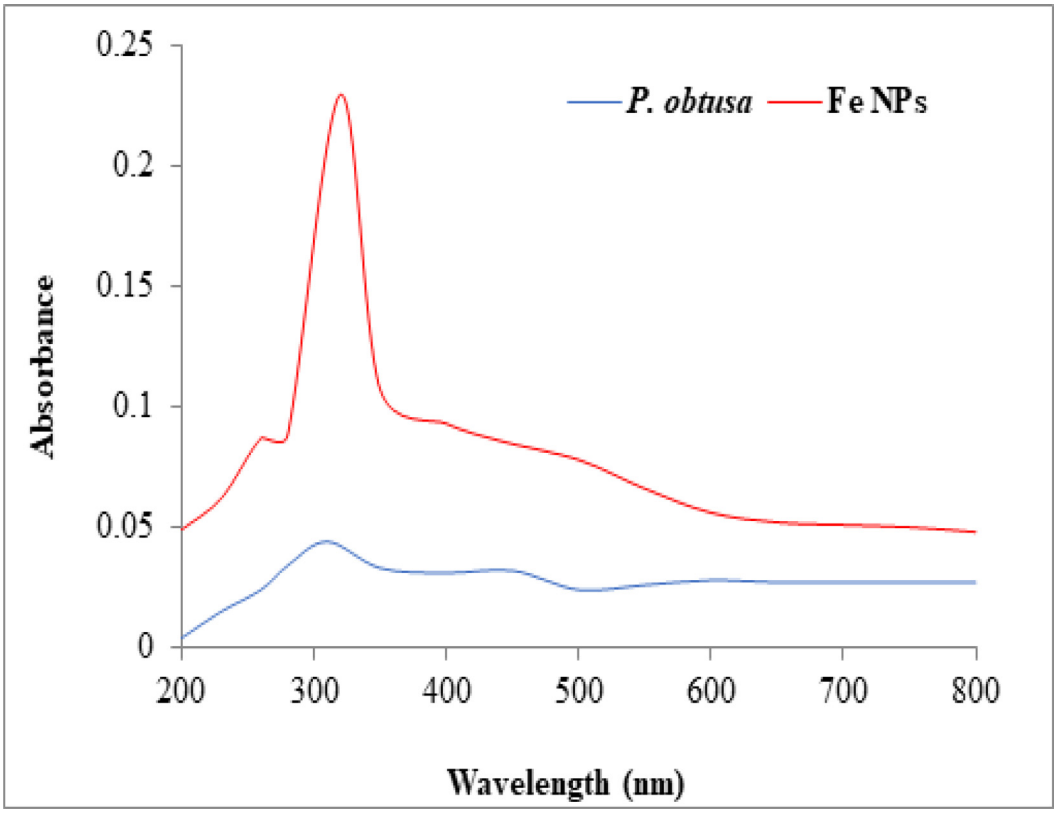

Fig. 2 UV/Visible spectra of *P. obtusa* extract and FeNPs.

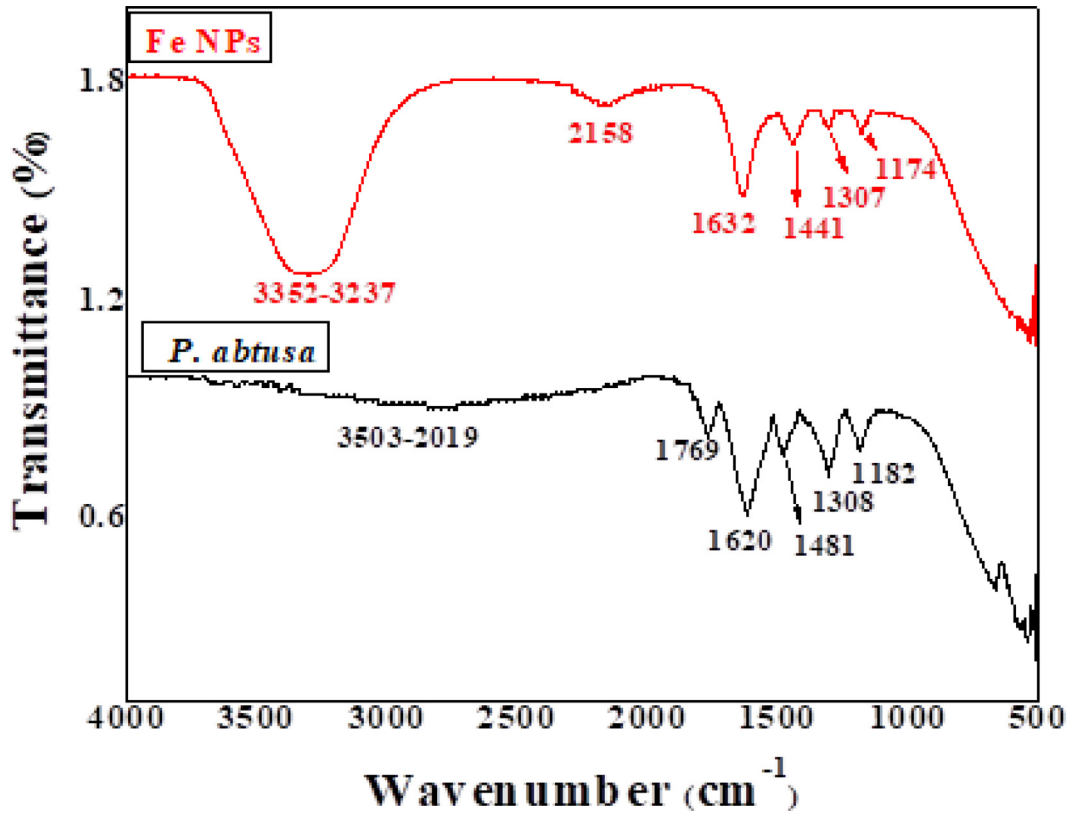

Fig. 3 FTIR spectra of FeNPs and *P. obtusa* extract.

on NPs were responsible for the biological activities of NPs (Al-Fa'ouri et al., 2021; Amer and Awwad, 2021; Shammout and Awwad, 2021).

The XRD analysis was performed to study structure of biosynthesized FeNPs. The Bragg peaks observed in *P. obtusa* mediated FeNPs were in agreement to pure phase of FeNPs that agree with JCPD: 95-905-1447. The FeNPs distinct XRD diffraction peaks were indexed at 2θ values of 10.46°, 15.8°, 29.22°, 35.14° and 40.59°, which representing (110), (200), (201), (211), (020) and (222) crystallographic planes, respectively (Fig. 4). The sharp XRD peaks showed highly crystalline nature of FeNPs. Scherer's approximation was used to calculate average size of FeNPs and it was found to be 50 nm. Fig. 5 depicts the SEM images of FeNPs of spherical shape. The FeNPs were also characterized using TEM in order to further elucidate morphology and size of NPs. The spherical shape of NPs was observed from TEM images as given in Fig. 6. These spectroscopic analysis are in closer agreement with previous reported (Khalil et al., 2017; Abbasi et al., 2019; Li et al., 2020).

3.2. Antimicrobial activity

Traditional medications available in pharmaceutical industries play imperative part to treat different microbial ailments, but are associated to problems, i.e., resistance against antibiotics. Hence, researchers are exploring the alternative ways to design alternate materials in order to combat against antibiotic resistance as well as to minimize the risks of spread of diseases (Patil Shriniwas, 2017; Abbasi et al., 2019). Thus, the advances in nano-biotechnology have opened the avenues for fabrication of advanced materials (metal NPs) with the special antimicrobial potential for biomedical applications.

The antibacterial activities of FeNPs and aqueous leave extract were executed by using bacterial strains viz. *E. coli* and *B. subtilis* and response are depicted in Fig. 7(a and b) and Fig. 8a. The antibacterial activity of *P. obtusa* leaves extract and different concentrations FeNPs was evaluated by disc diffusion method. The zone of inhibition (maximum) was observed at 100 µg/mL, 18 ± 0.03 mm and 16 ± 0.03 m m for extract of *P. obtusa* against *E. coli* and *B. subtilis,* respectively. Whereas, the highest inhibition zone in case of FeNPs (at 100 µg/mL) was 29 ± 0.03 mm against *E. coli* and 24 ± 0.04 mm against *B. subtilis*. At 100 µg/mL concentration, the standard (streptomycin) exhibited the zone of inhibition 24 ± 0.06 mm against *E. coli* and 22 ± 0.05 mm against *B. subtilis*. The FeNPs showed promising ($P < 0.01$) activity in comparison to standard. The bactericidal activity of FeNPs was due to the cations (Fe^{+2}) formation, which get inclined to the bacterial cell-wall having negative charge owing to electrostatic attractions. The FeNPs then further penetrate inside the bacteria thus inhibiting its growth. The NPs in the cytoplasm interact with biomolecules (-S- containing enzymes and proteins) as well as DNA and preclude them from the normal functioning inside the cell. Thus, resulting in complete destruction of bacterial cell (Khan et al., 2017; Abbasi et al., 2019; Iqbal et al., 2020). Besides, previous studies revealed that generation of ROS (reactive oxygen species) is the base of damage (oxidative) in bacterial cells for the NPs-based toxicity. Moreover, the defects (on the surface) of NPs also might account for cells injury and antibacterial growth inhibition. Furthermore, the bioactive on the exterior of FeNPs from

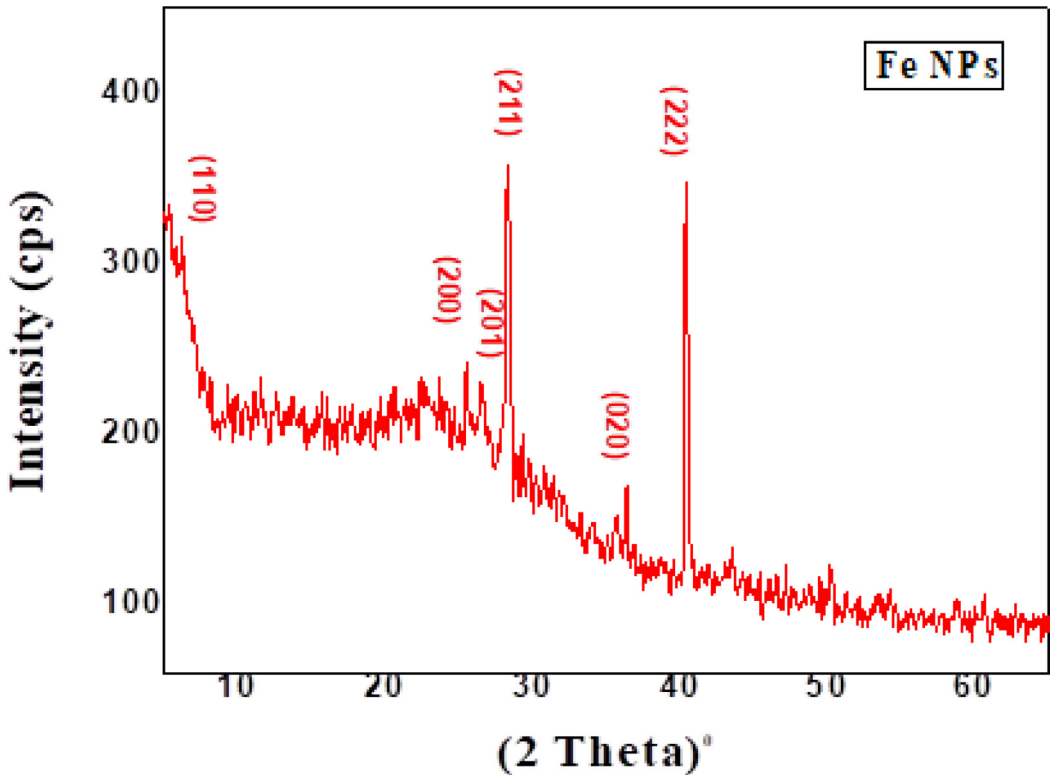

Fig. 4 XRD pattern of FeNPs synthesized using *P. obtusa* extract.

the extract used for stabilization and capping of NPs played significant antibacterial potential role (Abbasi et al., 2019; Ibrahim et al., 2021). The dose-dependent antibacterial activities of the present study are in agreement studies reported earlier [31,32].

The antifungal activities were assessed for both *P. obtusa* extract and FeNPs in 20–100 µg/mL and the findings are displayed in Figs. 7(c, d) and 8b. In case of *P. obtuse* extract, the obtained zones of inhibition were 14 ± 0.02 mm against *A. niger* and 17 ± 0.02 mm against *S. commune*. The FeNPs showed 24 ± 0.02 mm zones of inhibition against *A. niger* and 28 ± 0.03 mm against *S. commune* at 100 µg/mL concentration. The zone of inhibition exhibited by standard (fluconazole) against *A. niger* was 21 ± 0.05 mm, whereas it was 26 ± 0.4 mm against *S. commune*. A significantly antifungal activity ($P < 0.005$) was shown by FeNPs versus standard. The FeNPs furnished a dose-dependent activity and was enhanced markedly as the concentration of the NPs increased.

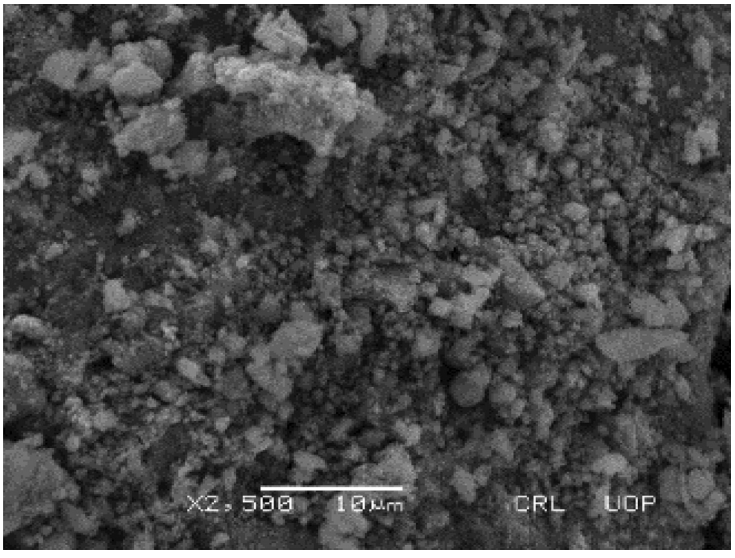

Fig. 5 SEM analysis of FeNPs synthesized using *P. obtusa* extract.

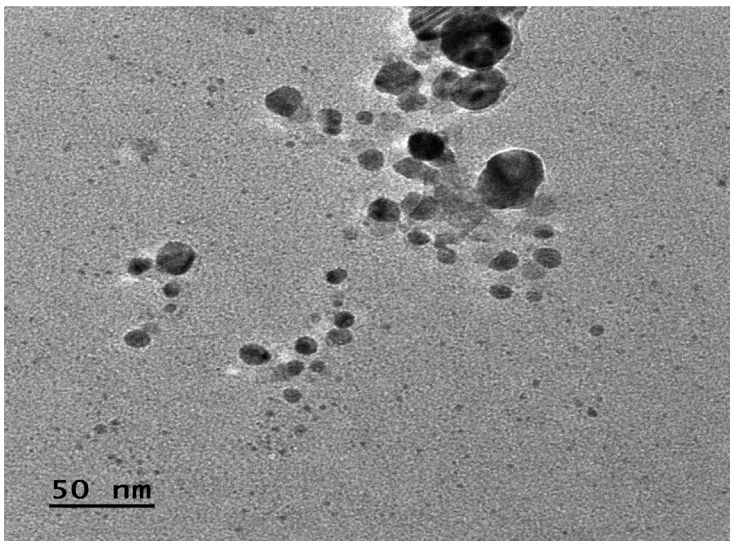

Fig. 6 TEM analysis of FeNPs synthesized using *P. obtusa* extract.

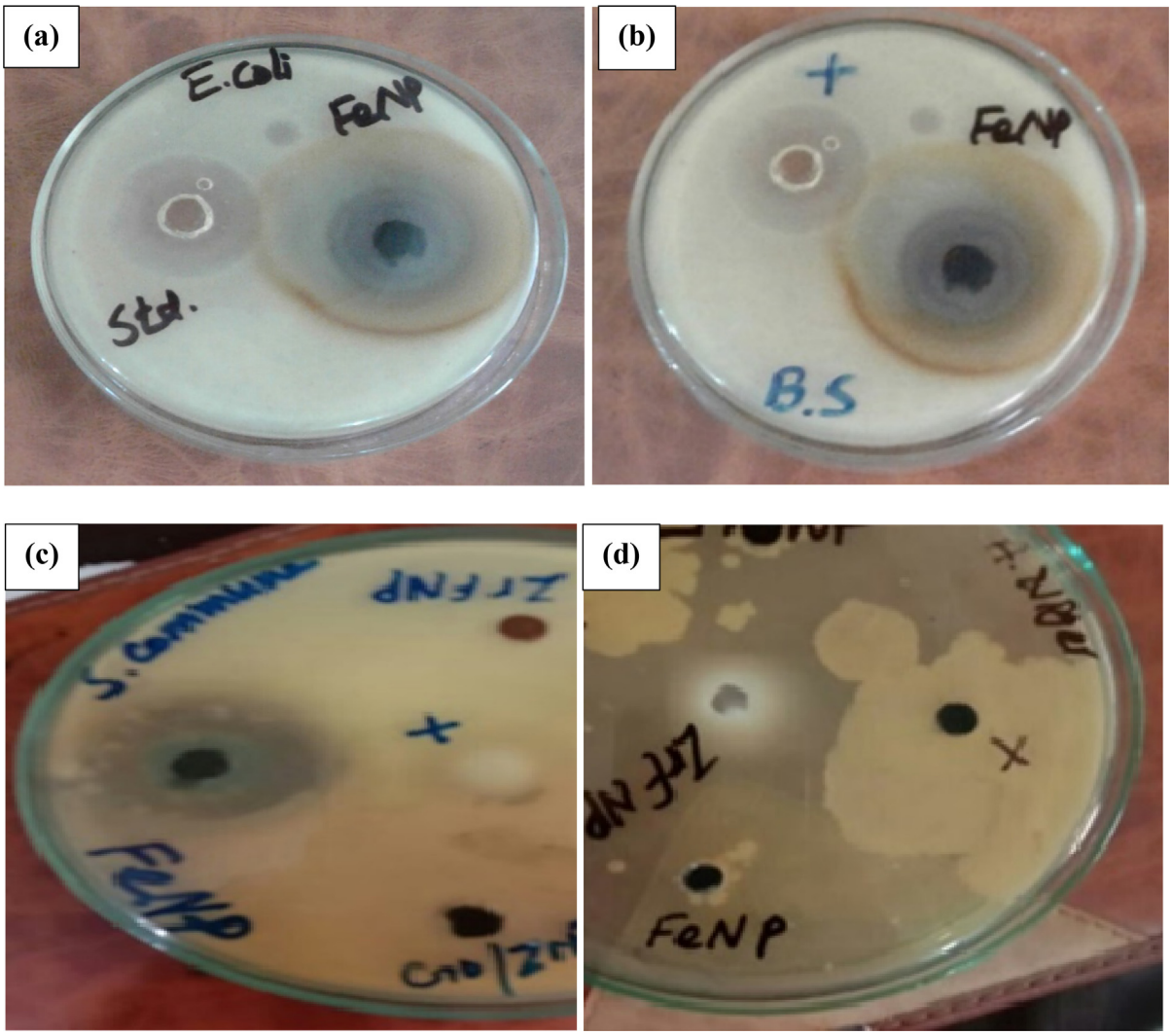

Fig. 7 Antimicrobial activity, zone of inhibition (mm), (a, b) against *E. coli*, *B. subtilis* and (c, d) against *S. commune* and *A. niger*.

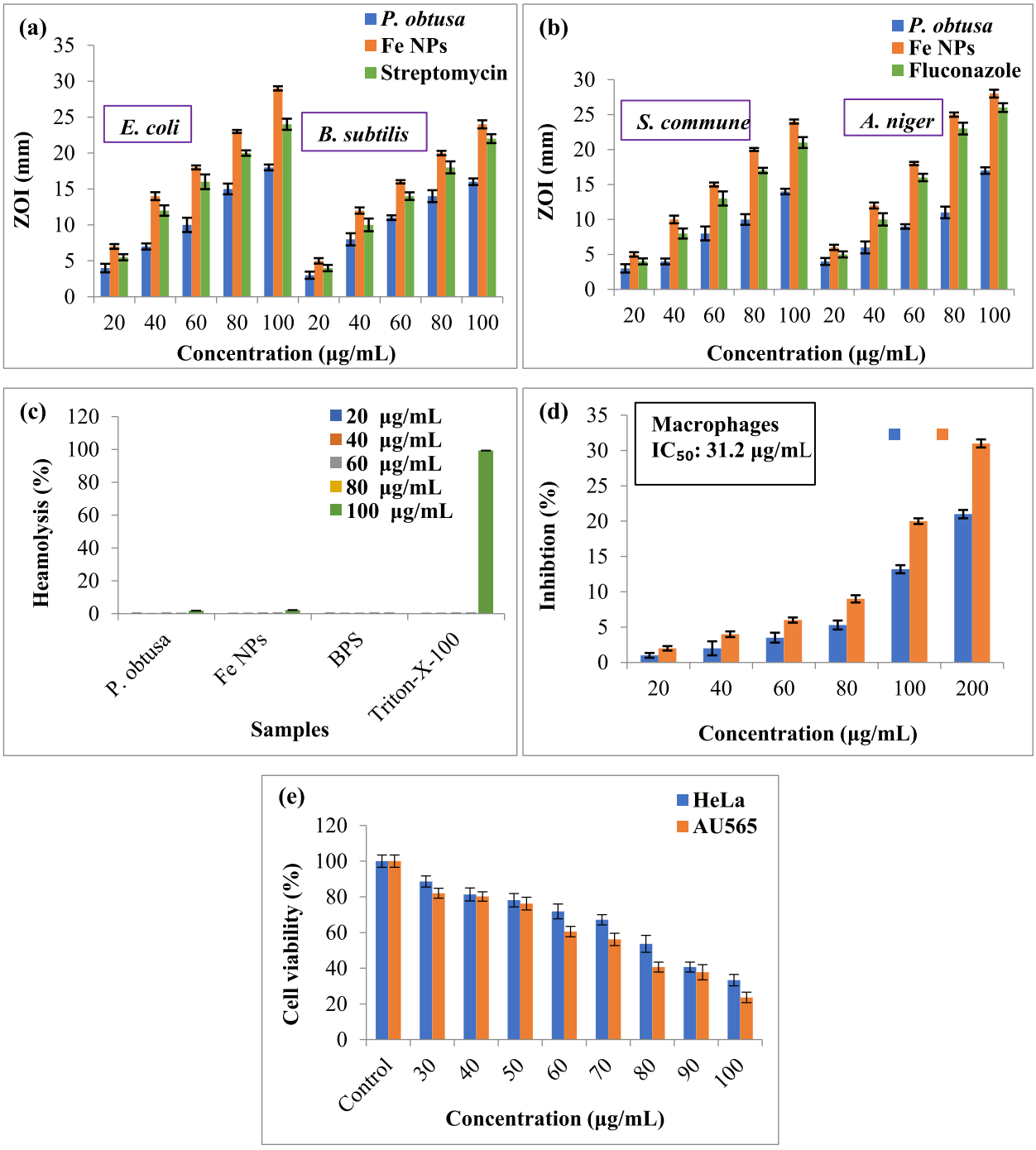

Fig. 8 (a) Antibacterial, (b) antifungal, (c) hemolytic activity, (d) biocompatibility against macrophages, (e) *in vitro* cytotoxicity exhibited by green synthesized FeNPs at different concentrations.

The FeNPs inhibition activity was due to its small particle size. The smaller sized FeNPs could penetrate in the lipid membrane easily consequently blocked the binding sites of fungal enzymes thus inhibited mycelial growth. The damage of cytoplasm by deteriorating the structure of fungus due to apoptosis. The previous reports suggested that the FeNPs interference with spores and hyphae of fungus, the generation of ROS also led to inhibition in growth of fungus (Abbasi et al., 2019, Iqbal et al., 2020; Wang et al., 2021). The antifungal characteristic exhibited by green synthesized metal NPs are very important candidate for the biological applications. These findings are in accordance with the earlier observations (Yadav and Fulekar, 2018; Abbasi et al., 2019; Ibrahim et al., 2021).

The MICs values were observed as 125 ± 0.11, 250 ± 0.09, 250 ± 0.13 and 125 ± 0.08 for *P. obtusa* and 62.5 ± 0.9, 31.25 ± 0.07, 62.5 ± 0.11 and 62.5 ± 0.12 µg/mL in case of FeNPs against *E. coli*, *B. subtilis*, *A. niger* and *S. commune* microbial strains, respectively. The MICs values of 63.4 ± 0.1, 32.31 ± 0.09, 61.95 ± 0.13 and 62.15 ± 0.08 (µg/mL) were observed against *E. coli*, *B. subtilis*, *A. niger* and *S. commune,* respectively

for standard drugs (streptomycin for bacterial strain and Fluconazole for fungal strain). All the results were statistically significant with probability value of $P < 0.005$. The MIC is defined as the visible inhibition of microorganism growth as an antimicrobial agent is added under definite conditions. The less MIC value indicates the higher activity of the NPs employed as antimicrobial agent. Lower values of MICs was observed in case of *P. obtusa* mediated FeNPs as compared to *P. obtusa* against these strains. The difference in MIC value of FeNPs and extract might be due to smaller size of NPs beside the bio-molecules nature in different plant extracts utilized for the formulation of FeNPs (Khan et al., 2017; Abbasi et al., 2019; Iqbal et al., 2020; Hasanin, 2021).

3.3. Cytotoxicity and biocompatibility

The toxicological and biocompatible nature of FeNPs was assessed against human macrophages and RBCs. According to the standard guidelines set by American Society, the biological substances are hemolytic if exposing the RBCs and its hemolysis greater than 5%, 2–5% are slightly hemolytic, while those having <2% are non-cytotoxic. The % hemolysis is the release of hemoglobin after rupturing of RBCs on treating with FeNPs. If tested NPs is hemolytic, it will rupture the RBCs and results in release of hemoglobin. The hemolytic assay of FeNPs was done against RBCs (human) in the range of 20–100 µg/mL as depicted in Fig. 8c. The *P. obtusa* showed 1.8 ± 0.01 and FeNPs 2.1 ± 0.01% hemolysis at 100 µg/mL and below this concentration no lysis was observed for both extract and NPs. The 100% lysis was examined for positive control (Triton-X-100), however 0% was observed for negative control (PBS). The presence of phyto-constituents in plant extract also plays a significant in biosafety of the NPs. Up to 2.1%, the RBCs lysis is due to the action of biomolecules that maintain RBCs membrane integrity by inhibiting oxidation phenomenon. In addition to this, the plasma antiradical activity also enhanced (Jamdagni et al., 2018; Abou-Yousef et al., 2021). This biocompatibility assessment is pivotal for understanding the cytotoxic behavior of NPs. Our studies concluded that biosynthesized FeNPs at low concentrations are non-hemolytic against RBCs, thus confirming their safe nature and biocompatible nature. Our findings are also consistent with earlier reports (Iqbal et al., 2019) who determined the hemolysis of RBCs using metal NPs synthesized using plant extract. There was no apparent lysis seen in RBCs on exposure of these metal NPs at low concentrations.

The MTT cytotoxic assay was performed to confirm the biosafety of FeNPs against human macrophages. The results of MTT assay showed inhibition response was dose-dependent. It was inferred from findings that macrophages response was higher on treating with FeNPs higher concentration, while cytotoxicity reduced at lower concentration. The results depicted in Fig. 8d revealed that 31.32 ± 0.04 and 21 ± 0.0.3% inhibition of *P. obtusa* and FeNPs in macrophages growth at 200 µg/mL concentration thus confirming the FeNPs non-toxic behavior ($P < 0.01$). The macrophage mechanism of FeNPs was to scavenge the ROS produced from external sources by its reduction. The FeNPs at low concentration were non-toxic to macrophages and human erythrocytes except its quantity enhanced beyond the threshold limit (Prach et al., 2013; Abou-Yousef et al., 2021).

The FeNPs were also analyzed against the AU565 and HeLa cell lines, the cell viability decreased as the concentration increased from 30 to 100 µg/mL. More cell decline observed in AU565 (82.03 ± 0.08 to 23.65 ± 0.065 %) with IC_{50} of 47.5 1 ± 0.08 µg/mL in comparison to the HeLa cell lines, in which the analyzed cell viability ranged from 88.61 ± 0.06 to 33.34 ± 0.06 % (IC_{50} 55.36 ± 0.07 µg/mL) (Fig. 8e). The cells retained intact and shown 100% cell viability without any treatment served as control. The HeLa cell lines results compared to Cisplatin (standard), which showed 97.15 ± 0.09% decline in viability of cells and another standard Doxorubicin employed for AU565 cell lines with 98.80 ± 0.09% cell viability was declined. The higher FeNPs concentration enhanced the cell viability loss in both cases. AU565 and HeLa cell lines show decreased cell viability at higher concentration, but the extent was observed to be different in the two cell lines. This difference indicates the more resistant nature of HeLa cell lines under similar conditions as compared to AU565. The FeNPs IC_{50} value was recorded to be 371.3 µg/mL. The findings of biocompatibility, i.e., hemolytic ($P < 0.01$), microphages ($P < 0.01$), cell lines ($P < 0.01$) showed significant values at 100 µg/mL concentration of FeNPs. Similarly, (Rajan et al., 2017; Dacrory et al., 2021) studied the cytotoxicity of NPs from *E. cardamomum* extract against HeLa cell lines and an increased activity shown was observed in concentration dependent manner.

3.4. Antioxidant activities

The reactive oxygen species (ROS) in living organism cause membrane damage via lipid oxidation resulting in various ailments. Plant mediated metal NPs have potential to scavenge these ROS. Since *P. obtusa* leaf extract mediated FeNPs was used in present study as strong capping and reducing agent. It is assumed, that some flavonoids quench ROS on the surface of FeNPs (Khan et al., 2017; Abbasi et al., 2019; Iqbal et al., 2020; Hasanin 2021). The antioxidant activities like total reducing power ability DPPHH_2O_2 and NO of *P. obtusa* mediated FeNPs were evaluated at different concentrations. The findings of DPPH scavenging for different concentration of FeNPs as % inhibition values at concentration 25–500 µg/mL are presented in Fig. 9a. The results revealed that DPPH radical scavenging potential values as 56.34 ± 0.03% for *P. obtuse,* while 70.23 ± 0.02% for FeNPs at concentration 500 µg/mL, respectively. The radical scavenging potential of ascorbic acid (standard) determined was 66 ± 0.02%. It was found that % inhibition increases by increasing the concentration. The FeNPs showed significant scavenging activity and results were comparable to the standard. It was deduced that free radicals such as DPPH has central nitrogen having ability to accept hydrogen radical or electron and some antioxidants compound in extract and NPs might involve in reducing the free radicals. The purple-colored DPPH solution turned yellow during the reduction of DPPH radical to non-radical form. The absorption for this reduction was determined at 517 nm which indicated strong antioxidant potential (Abbasi et al., 2019; Dacrory et al., 2021).

The antioxidant potential of leaves extract and FeNPs in concentration range of 25–250 µg/mL was investigated using total reducing power ability (TRPA). The reducing power ability values observed in case of *P. obtusa* extract was 67.46 ± 0.

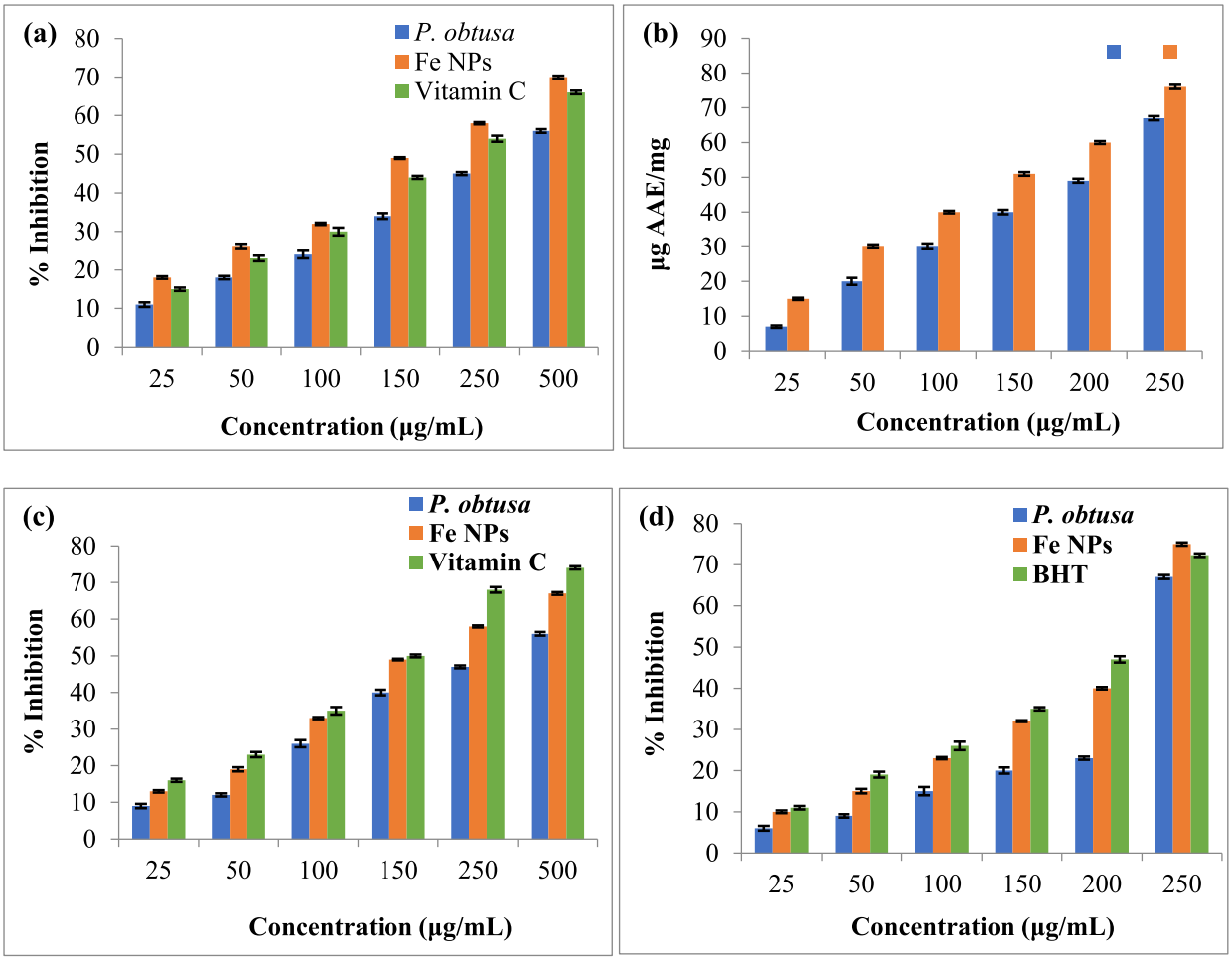

Fig. 9 (a) DPPH, (b) TRPA, (c) H_2O_2, (d) NO radical scavenging activities at different concentrations of extract and FeNPs.

03 µg AAE/mg, these values were 76.65 ± 0.02 µg AAE/mg in case of FeNPs at 250 µg/mL. The findings revealed that *P. obtusa* mediated FeNPs showed strong antioxidant activity in concentration dependent way (Fig. 9b). The mechanism for TRPA activity was the involvement of the reduction in antioxidant potentials of FeNPs by providing H-atom that quench the free radical chain. When compared to plant extract, the activity was significant of biosynthesized NPs. Ferrous ions (Fe^{2+}) are obtained from the ferricyanide complex (Fe^{3+}) during this assay as evident from the change in color from yellow to bluish green (Abbasi et al., 2019).

The inhibition of H_2O_2 radical scavenging responses have been shown in Fig. 9c for the concentration range of 25–500 µg/mL. The radical scavenging was enhanced in a dose dependent manner, i.e., maximum radical quenching was observed at 500 µg/mL that was 56.82 ± 0.02% for *P. obtusa* extract and 67.34 ± 0.02% in case FeNPs. The values of H_2O_2 radical scavenging for standard (ascorbic acid) was 74 ± 0.02%. The phenomenon of aging and other similar disorder are associated with the generation of free radicals including H_2O_2, which disturb the numerous energy producing systems. The NPs have strong ability to scavenge these radicals and exhibited antioxidant potential, which increased with concentration (Patil Shriniwas, 2017; Abu-Elghait et al., 2021).

The NO radical scavenging activity was evaluated at concentrations (25–250 µg/mL), *P. obtusa* showed inhibition of 67.08 ± 0.03%, whereas FeNPs showed 74.43 ± 0.02% at 250 µg/mL concentration (Fig. 9d). The BHT (butylated hydrogen toluene) was employed as a standard to test NO scavenging potential, which showed 72.3 ± 0.02% NO radical scavenging activity. The biosynthesized FeNPs exhibited strong scavenging ability. The NO is involved in many biological functions including neuro transmission, antimicrobial, anticancer properties and smooth muscle relaxation in addition to regulation of blood pressure (Khan et al., 2017). The reaction of NO with superoxide produces peroxynitrite anion, which result in oxidation of lipids and DNA fragmentation responsible for oxidative damage. The NO regularization should be managed to avoid its harmful effects and scavenging through NPs quite significant in this regard (Patil Shriniwas, 2017; Abu-Elghait et al., 2021). The FeNPs exhibited significant free radical scavenging potential for assays performed viz. TRPA ($P < 0.01$), DPPH ($P < 0.005$), H_2O_2 ($P < 0.05$) and NO ($P < 0.001$) for DPPH and H_2O_2 the concentration was 500 µg/mL and 250 µg/mL for TRPA and NO. The FeNPs proved to be promising for biomedical applications since the DPPH, TRPA, H2O2 and NO showed the potential activity and also previous findings are in line for NPs biosynthesized using *Callistemon viminalis*, *Rhamnus virgata* and *Fagonia*

indica (Khan et al., 2017). Also green route for the fabrication NP is eco-benign and facile versus other physicochemical approaches (Remya et al., 2017; Al Banna et al., 2020; Awwad et al., 2020; Fatima et al., 2020; Amer and Awwad, 2021; Shahid et al., 2021).

4. Conclusions

The green synthesis of FeNPs using leaves extract of *Plumeria obtusa* was an efficient, cost effective, ecofriendly and facile approach. The green synthesized FeNPs were characterized via different microscopic and spectroscopic techniques in order to elucidate functionality, stability and size of NPs. The FeNPs were obtained at nanoscale with spherical shape and crystalline nature. Furthermore, the antimicrobial activity of this FeNPs against fungal and bacterial stains was evaluated, which was promising and FeNPs concentration dependent. Moreover, FeNPs was non-toxic for RBCs up to 100 µg/mL. The antioxidant potential of was promising and observed in concentration dependent. The FeNPs can be a potential candidate as a preventive and therapeutic drug against microbes. In future consideration, the evolution of disease resistance to currently available drugs, green synthesis is a way forward to design novel nano-medicine that might serve for both to diagnose as well as treat different ailments. Further *in vivo* study is encouraged for toxicological aspects on animal models.

Funding

Higher Education commission of Pakistan is acknowledged for providing research facilities viz. grant TDF-02-153. Princess Nourah bint Abdulrahman University Researchers Supporting Project number (PNURSP2022R158) Princess Nourah bint Abdulrahman University, Riyadh, Saudi Arabia. The authors extend their appreciation to the Deanship of Scientific Research at King Khalid University, Saudi Arabia for funding this work through Research Groups Program under grant number R.G.P.1: 229/43.

Acknowledgements

Higher Education commission of Pakistan is acknowledged for providing research facilities viz. grant TDF-02-153. Princess Nourah bint Abdulrahman University Researchers Supporting Project number (PNURSP2022R158) Princess Nourah bint Abdulrahman University, Riyadh, Saudi Arabia. The authors extend their appreciation to the Deanship of Scientific Research at King Khalid University, Saudi Arabia for funding this work through Research Groups Program under grant number R.G.P.1: 229/43.

References

Abbasi, B.A., Iqbal, J., Mahmood, T., et al, 2019. Biofabrication of iron oxide nanoparticles by leaf extract of Rhamnus virgata: characterization and evaluation of cytotoxic, antimicrobial and antioxidant potentials. Appl. Organometal. Chem. 33, e4947.

Abou-Yousef, H., Dacrory, S., Hasanin, M., et al, 2021. Biocompatible hydrogel based on aldehyde-functionalized cellulose and chitosan for potential control drug release. Sustain. Chem. Pharm. 21, 100419.

Abu-Elghait, M., Hasanin, M., Hashem, A.H., et al, 2021. Ecofriendly novel synthesis of tertiary composite based on cellulose and myco-synthesized selenium nanoparticles: Characterization, antibiofilm and biocompatibility. Int. J. Biol. Macromol. 175, 294–303.

Al-Fa'ouri, A.M., Abu-Kharma, M.H., Awwad, A.M., 2021. Green synthesis of copper oxide nanoparticles using Bougainvillea leaves aqueous extract and antibacterial activity evaluation. Chem. Int. 7, 155–162.

Al Banna, L.S., Salem, N.M., Jaleel, G.A., et al, 2020. Green synthesis of sulfur nanoparticles using Rosmarinus officinalis leaves extract and nematicidal activity against Meloidogyne javanica. Chem. Int. 6, 137–143.

Ali, S., Iqbal, M., Naseer, A., et al, 2021. State of the art of gold (Au) nanoparticles synthesis via green routes and applications: a review. Environ. Nanotechnol. Monit. Manage. 16, 100511.

Amer, M.W., Awwad, A.M., 2021. Green synthesis of copper nanoparticles by *Citrus limon* fruits extract, characterization and antibacterial activity. Chem. Int. 7, 1–8.

Awwad, A.M., Amer, M.W., 2020. Biosynthesis of copper oxide nanoparticles using Ailanthus altissima leaf extract and antibacterial activity. Chem. Int. 6, 210–217.

Awwad, A.M., Amer, M.W., Salem, N.M., et al, 2020a. Green synthesis of zinc oxide nanoparticles (ZnO-NPs) using Ailanthus altissima fruit extracts and antibacterial activity. Chem. Int. 6, 151–159.

Awwad, A.M., Salem, N.M., Aqarbeh, M.M., et al, 2020b. Green synthesis, characterization of silver sulfide nanoparticles and antibacterial activity evaluation. Chem. Int. 6, 42–48.

Bhatti, H.N., Iram, Z., Iqbal, M., et al, 2020. Facile synthesis of zero valent iron and photocatalytic application for the degradation of dyes. Mater. Res. Exp. 7, 015802.

Bibi, I., Nazar, N., Ata, S., et al, 2019. Green synthesis of iron oxide nanoparticles using pomegranate seeds extract and photocatalytic activity evaluation for the degradation of textile dye. J. Mater. Res. Technol. 8, 6115–6124.

Bihani, T., Mhaske, N., 2020. Evaluation of in vivo wound healing activity of Plumeria obtusa L. (Champa) spray in rats. Wound Med. 28, 100176.

Bihani, T., Tandel, P., Wadekar, J., 2021a. Plumeria obtusa L.: a systematic review of its traditional uses, morphology, phytochemistry and pharmacology. Phytomed. Plus., 100052

Bihani, T., Tandel, P., Wadekar, J., 2021b. Plumeria obtusa L.: a systematic review of its traditional uses, morphology, phytochemistry and pharmacology. Phytomed. Plus. 1, 100052.

Dacrory, S., Hashem, A.H., Hasanin, M., 2021. Synthesis of cellulose based amino acid functionalized nano-biocomplex: Characterization, antifungal activity, molecular docking and hemocompatibility. Environ. Nanotechnol. Monit. Manage. 15, 100453.

Fatima, S., Bhatti, H.N., Iqbal, M.A., et al, 2020. Synthesis of needle like Mn-Zn bimetallic nanoparticles and its applications towards photocatalysis and as fuel additives. Int. J. Environ. Anal. Chem., 1–16

Halanayake, K.D., Kalutharage, N.K., Hewage, J.W., 2021. Microencapsulation of biosynthesized zinc oxide nanoparticles (ZnO-NPs) using Plumeria leaf extract and kinetic studies in the release of ZnO-NPs from microcapsules. SN Appl. Sci. 3, 1–12.

Hamelian, M., Zangeneh, M.M., Amisama, A., et al, 2018. Green synthesis of silver nanoparticles using Thymus kotschyanus extract and evaluation of their antioxidant, antibacterial and cytotoxic effects. Appl. Organometal. Chem. 32, e4458.

Hasanin, M.S., 2021. Simple, economic, ecofriendly method to extract starch nanoparticles from potato peel waste for biological applications. Starch-Stärke., 2100055

Ibrahim, S., Elsayed, H., Hasanin, M., 2021. Biodegradable, antimicrobial and antioxidant biofilm for active packaging based on extracted gelatin and lignocelluloses biowastes. J. Polym. Environ. 29, 472–482.

Igwe, O.U., Nwamezie, F., 2018. Green synthesis of iron nanoparticles using flower extract of Piliostigma thonningii and antibacterial activity evaluation. Chem. Int. 4, 60–66.

Iqbal, J., Abbasi, B.A., Ahmad, R., et al, 2020. Biogenic synthesis of green and cost effective iron nanoparticles and evaluation of their potential biomedical properties. J. Mol. Struct. 1199, 126979.

Iqbal, J., Abbasi, B.A., Mahmood, T., et al, 2019. Plant-extract mediated green approach for the synthesis of ZnONPs: Characterization and evaluation of cytotoxic, antimicrobial and antioxidant potentials. J. Mol. Struct. 1189, 315–327.

Jamdagni, P., Khatri, P., Rana, J., 2018. Green synthesis of zinc oxide nanoparticles using flower extract of Nyctanthes arbor-tristis and their antifungal activity. J. King Saud Uni.-Sci. 30, 168–175.

Kamran, R.M., Khaliq, H.A., Uzair, M., 2020. Pharmacognostic and phytochemical studies on Plumeria obtusa L. J. Phytopharmacol. 9, 120–124.

Kamran, U., Bhatti, H.N., Iqbal, M., et al, 2019. Green synthesis of metal nanoparticles and their applications in different fields: a review. Z. Phys. Chem. 233, 1325–1349.

Khalil, A.T., Ovais, M., Ullah, I., et al, 2017. Biosynthesis of iron oxide (Fe2O3) nanoparticles via aqueous extracts of Sageretia thea (Osbeck.) and their pharmacognostic properties. Green Chem. Lett. Rev. 10, 186–201.

Khan, A., Anand, V., Badrinarayanan, V., et al, 2017. In vitro antioxidant and cytotoxicity analysis of leaves of Ficus racemosa. Free Rad. Antioxid. 7, 8–12.

Li, Y.-X., Zhang, C., Pan, S., et al, 2020. Analysis of chemical components and biological activities of essential oils from black and white pepper (Piper nigrum L.) in five provinces of southern China. LWT 117, 108644.

Nadeem, F., Bhatti, I., Ashar, A., et al, 2021. Eco-benign biodiesel production from waste cooking oil using eggshell derived MM-CaO catalyst and condition optimization using RSM approach. Arab. J. Chem. 14, 103263.

Nadhe, S.B., Tawre, M.S., Agrawal, S., et al, 2020. Anticancer potential of AgNPs synthesized using Acinetobacter sp. and Curcuma aromatica against HeLa cell lines: a comparative study. J. Trace Element Med. Biol. 62, 126630.

Naseer, A., Ali, A., Ali, S., et al, 2020. Biogenic and eco-benign synthesis of platinum nanoparticles (Pt NPs) using plants aqueous extracts and biological derivatives: environmental, biological and catalytic applications. J. Mater. Res. Technol. 9, 9093–9107.

Nazir, A., Akbar, A., Baghdadi, H.B., et al, 2021. Zinc oxide nanoparticles fabrication using Eriobotrya japonica leaves extract: photocatalytic performance and antibacterial activity evaluation. Arab. J. Chem. 14, 103251.

Noreen, S., Ismail, S., Ibrahim, S.M., et al, 2020a. ZnO, CuO and Fe2O3 green synthesis for the adsorptive removal of direct golden yellow dye adsorption: kinetics, equilibrium and thermodynamics studies. Z. Phys. Chem. 235, 1055–1075.

Noreen, S., Mustafa, G., Ibrahim, S.M., et al, 2020b. Iron oxide (Fe2O3) prepared via green route and adsorption efficiency evaluation for an anionic dye: kinetics, isotherms and thermodynamics studies. J. Mater. Res. Technol. 9, 4206–4217.

Patil Shriniwas, P., 2017. Antioxidant, antibacterial and cytotoxic potential of silver nanoparticles synthesized using terpenes rich extract of Lantana camara L. leaves. Biochem. Biophys. Report. 10, 76.

Prach, M., Stone, V., Proudfoot, L., 2013. Zinc oxide nanoparticles and monocytes: impact of size, charge and solubility on activation status. Toxicol. Appl. Pharmacol. 266, 19–26.

Rahmat, M., Bhatti, H.N., Rehman, A., et al, 2021. Bionanocomposite of Au decorated MnO2 via in situ green synthesis route and antimicrobial activity evaluation. Arab. J Chem., 103415

Rajan, A., Rajan, A.R., Philip, D., 2017. Elettaria cardamomum seed mediated rapid synthesis of gold nanoparticles and its biological activities. OpenNano 2, 1–8.

Remya, V., Abitha, V., Rajput, P., et al, 2017. Silver nanoparticles green synthesis: a mini review. Chem. Int. 3, 165–171.

Rolim, W.R., Pelegrino, M.T., de Araújo Lima, B., et al, 2019. Green tea extract mediated biogenic synthesis of silver nanoparticles: characterization, cytotoxicity evaluation and antibacterial activity. Appl. Surf. Sci. 463, 66–74.

Ruan, H., Wu, X., Yang, C., et al, 2018. A supersensitive CTC analysis system based on triangular silver nanoprisms and SPION with function of capture, enrichment, detection, and release. ACS Biomater. Sci. Eng. 4, 1073–1082.

Sangaonkar, G.M., Pawar, K.D., 2018. Garcinia indica mediated biogenic synthesis of silver nanoparticles with antibacterial and antioxidant activities. Colloid. Surf. B. 164, 210–217.

Shahid, M., Munir, H., Akhter, N., et al, 2021. Nanoparticles encapsulation of Phoenix dactylifera (date palm) mucilage for colonic drug delivery. Int. J. Biol. Macromol. 191, 861–871.

Shammout, M.W., Awwad, A.M., 2021. A novel route for the synthesis of copper oxide nanoparticles using Bougainvillea plant flowers extract and antifungal activity evaluation. Chem. Int. 7, 71–78.

Wang, Y., Wang, L., Tan, J., et al, 2021. Comparative analysis of intracellular and in vitro antioxidant activities of essential oil from white and black pepper (Piper nigrum L.). Front. Pharmacol. 12, 1344.

Yadav, V.K., Fulekar, M., 2018. Biogenic synthesis of maghemite nanoparticles (γ-Fe2O3) using Tridax leaf extract and its application for removal of fly ash heavy metals (Pb, Cd). Mater. Today: Proc. 5, 20704–20710.